

Influence of Ethylene and Acetylene on the Rate and Reversibility of Methane Dehydroaromatization on Mo/H-ZSM-5 Catalysts

Neil K. Razdan, Anurag Kumar, Brandon L. Foley, and Aditya Bhan*

Department of Chemical Engineering and Materials Science, University of Minnesota-Twin Cities, 421 Washington Avenue SE, Minneapolis, Minnesota 55455, United States

*Corresponding Author: E-mail: abhan@umn.edu; Fax: (+1) 612-626-7246

Abstract

Acetylene is identified as a key intermediate in methane dehydroaromatization (DHA) reactions present in concentrations $\mathcal{O}(1)$ Pascal. The rank of acetylene and other C_2 hydrocarbon intermediates is determined by conversion-selectivity profiles collected from 0.01-8% methane conversion varied by extent of “non-selective” deactivation of Mo/H-ZSM-5 catalysts. Ethane is shown to be the sole primary product of methane pyrolysis and is sequentially dehydrogenated to ethylene and acetylene – which aromatizes to benzene with rates similar to direct acetylene aromatization measured in the absence of methane. The influence of C-H cleavage and C-C coupling events to control the rate and reversibility of DHA is assessed by the degree of reversibility control, introduced here for the first time, and the degree of rate control. The approach to equilibrium of the methane to benzene synthesis reaction is length averaged and affinity averaged by the degree of reversibility control of each intervening elementary step to rigorously calculate forward rates of benzene synthesis by use of De Donder relations. Forward rates are found to be invariant along the catalyst bed once the DHA network reaches a pseudo-steady state and methane, ethane, and ethylene form an equilibrated pool.

Keywords: Dehydroaromatization, Methane conversion, De Donder relations, Microscopic reversibility, Degree of rate control, Degree of reversibility control, H-ZSM-5, Molybdenum carbide

1. Introduction

Strong, apolar C-H bonds in methane confer significant thermodynamic and kinetic challenges in non-oxidative methane valorization [1,2]. Mo-modified medium pore MFI zeolites (Mo/H-ZSM-5) reduce kinetic barriers to methane pyrolysis and catalyze dehydroaromatization (DHA) reactions with high benzene ($\geq 70\%$) and aromatic ($\geq 95\%$) selectivity [3–7]. Active Mo/H-ZSM-5 catalysts contain carbidic forms of Mo synthesized from high-temperature (~ 950 K) reduction and carburization of oxidic Mo precursors impregnated within ZSM-5 zeolite by

either incipient wetness impregnation or vapor-phase cation exchange. Preparation of oxidic “pre-catalysts” by solid-state vapor-phase exchange of MoO_3 monomers with proximate pairs of zeolitic Brønsted acid sites in ZSM-5 anchors Mo cations to the zeolite framework as well-defined $(\text{Mo}_2\text{O}_5)^{2+}$ dimers [8,9]. Impregnation of oxidic Mo, provenance of dimeric $(\text{Mo}_2\text{O}_5)^{2+}$, and evolution to carbidic Mo by carburization in methane is confirmed by Raman spectroscopy, infrared absorption (IR), X-ray absorption spectroscopy, ^{27}Al magic-angle-spinning (MAS) NMR, transmission electron microscopy, and chemical transients during dimer formation and subsequent carburization [6,7,9–12]. These methods note evolution of $(\text{Mo}_2\text{O}_5)^{2+}$ to MoC_x , but do not probe stoichiometry or speciation of resultant carbidic Mo. Recent studies utilize ^{13}C MAS NMR, CO IR, and dynamic nuclear polarization surface enhanced NMR spectroscopy to show Mo speciation after carburization is diverse – including monomeric and dimeric (oxy)carbides and Mo_2C nanoparticles which may all play some catalytic role [13–16].

Even at high DHA reaction temperatures (~ 950 K), thermodynamic barriers to methane valorization persist, limiting equilibrium conversion to $\sim 10\%$ [17–22]. Stringent thermodynamic constraints result in a highly reversible DHA reaction network with observed net benzene synthesis rates decreasing with catalyst contact time as reverse hydrogenation and cracking reactions become prominent [6]. In this study we seek to evaluate the intrinsic kinetics of methane DHA on Mo/H-ZSM-5 by quantitatively accounting for the influence of reverse reactions on observed net rates. We rigorously de-convolute thermodynamic and kinetic contributions to observed DHA rates in order to (i) elucidate the rate control of intervening dehydrogenation and oligomerization events, and (ii) isolate the forward rate of benzene formation on Mo/H-ZSM-5. Application of De Donder relations and concepts of microscopic reversibility shows methane, ethane, and ethylene form an equilibrated pool at early contact

times corresponding to methane conversion $\geq 2.5\%$, congruent with existing reports [23,24], and reveals acetylene to be a key reactive intermediate in benzene formation, as suggested previously [25,26]. Elucidation of the DHA reaction network informs calculation of forward rates by allowing for quantitative appraisal of the reversibility of the single-path methane to benzene series reaction in terms of approach to equilibrium of constituent elementary steps. Previous investigations attempt to account for reversibility of the DHA reaction network by quantifying solely the approach to equilibrium of the overall benzene synthesis reaction ($6\text{CH}_4 \rightleftharpoons \text{C}_6\text{H}_6 + 9\text{H}_2$) [6,27]; however, we demonstrate the hitherto unrecognized importance of averaging reaction reversibility by the affinity of all non-equilibrated intervening steps during methane DHA. Determination of elementary step reversibilities permits quantitative appraisal of kinetic and thermodynamic influence of dehydrogenation and oligomerization events in terms of the degree of rate control and the degree of reversibility control, defined herein for the first time. Finally, we outline and address the critical importance of formalisms of affinity averaging and spatial averaging to calculate forward rates in flow reactors. We rigorously affinity average and spatially average overall approach to equilibrium of benzene synthesis to demonstrate forward aromatization rates are invariant once a pseudo-steady state is achieved upon equilibration of methane, ethane, and ethylene.

2. Materials and Methods

2.1 Catalyst synthesis and preparation

Mo/H-ZSM-5 catalysts were synthesized by exposure of MoO_x/H-ZSM-5 “pre-catalysts” to 0.21 cm³ s⁻¹ 90% CH₄ at 973 K and ~115 kPa total pressure, irrespective of catalyst loading or total flow rate during DHA reactions. MoO_x/H-ZSM-5 materials were prepared by methods detailed previously [6,7,12,28,29] and summarized in the following. In brief, H-ZSM-5 zeolite

was synthesized from NH₄-ZSM-5 (Zeolyst International, Si/Al = 11.5, CBV 2314) treated in dry air (~1.67 cm³ s⁻¹) to thermally decompose NH₄⁺ to H⁺ and NH₃(g) at 773 K (0.0165 K s⁻¹; 36 h hold). Oxidic Mo precursors, MoO₃ (Sigma-Aldrich, 99.9%), were physically mixed with H-ZSM-5 powders in an agate mortar and pestle for 15-30 min with nominally 3.3 wt% Mo (Mo/Al = 0.25). Intimate MoO₃ + H-ZSM-5 mixtures were heated from ambient temperature to 623 K (0.0167 K s⁻¹) and held for 15 h in dry air (0.67 cm³ s⁻¹) to ensure removal of physisorbed water and dispersion of MoO_x oligomers on the external zeolite surface [8–10]. Solid-state vapor-phase exchange of oxidic Mo with zeolitic Brønsted acid sites was achieved at 973 K (0.167 K s⁻¹; 10 h hold). The resultant MoO_x/H-ZSM-5 material was pressed, crushed, and sieved to obtain particle sizes between 180 and 425 μm (mesh 40 – 80) for activation to Mo/H-ZSM-5 and use in catalytic dehydroaromatization reactions.

2.2 Methane dehydroaromatization catalytic reactions

Methane dehydroaromatization reactions were performed in fixed-bed tubular quartz reactors (I.D. 10.5 mm). MoO_x/H-ZSM-5 materials were heated in inert He flow (~ 0.33 cm³ s⁻¹, UHP, Minneapolis Oxygen) to 973K at 0.18 K s⁻¹ in a resistively-heated furnace (National Element FA120). Tubular reactors were encased in an annular Inconel cylinder to ensure gradientless conduction of heat between the furnace and quartz reactor. Catalyst-bed temperature was monitored by two thermocouples stationed diametrically on the outer wall of the tubular quartz reactor. Oxidic pre-catalysts were exposed to CH₄/Ar (90 vol% CH₄ and 10 vol% Ar, total feed flow rate 0.21 cm³ s⁻¹, UHP, Matheson Tri-Gas) at 973 K until carburization is complete – as indicated by closure of carbon balance. Illustrative data is shown in Section S1. DHA reactions were either continued under 0.21 cm³ s⁻¹ total flow or were performed at identical composition, but varied flow range (0.21-2.1 cm³ s⁻¹), after ~30 minutes flush of reactor lines in He flow (~

0.33 cm³ s⁻¹) as reaction feed flow stabilized. Entrance and exit flow lines were heated to > 450K via resistive-heating tapes to prevent condensation of aromatic products and water. The effluent composition was analyzed using a mass spectrometer (MKS Cirrus 200 Quadrupole MS system) and a gas chromatograph (Agilent 7890) equipped with a methyl-siloxane capillary column (HP-1, 50 m x 320 μm x 0.52 μm) connected to a flame ionization detector (FID) for detection of hydrocarbons and a GS-GasPro column (60 m x 0.320 mm) connected to a thermal conductivity detector (TCD) for detection of permanent gases (H₂, Ar, and CH₄).

3. Results and Discussion

Methane dehydroaromatization reactions were performed over 0.025-1.2 g of Mo/H-ZSM-5 (Mo/Al = 0.25, Si/Al = 11.5) catalysts at 973 K with 0.21-2.1 cm³ s⁻¹ total flow of 90% CH₄ and 10% Ar as an internal standard at ~115 kPa total pressure. All reported flow rates are at standard temperature and pressure (STP).

3.1 Methane DHA reaction pathway

Figure 1 shows selectivities of DHA products as a function of methane conversion over several Mo/H-ZSM-5 catalyst samples at 973 K. Changes in conversion for each catalyst sample are achieved by allowing the catalyst to deactivate with time on stream (TOS). The coincidence of conversion-selectivity profiles for each product across three samples and 0.5-8% methane conversion, *f*, demonstrates that deactivation of Mo/H-ZSM-5 catalysts is “non-selective”, or occurs without modification of the intrinsic chemical nature of catalytic sites [10,30,31]. Thus, elucidation of the DHA reaction network by contact-time variation experiments at steady state can equivalently be performed by allowing Mo/H-ZSM-5 catalysts to deactivate with time on stream.

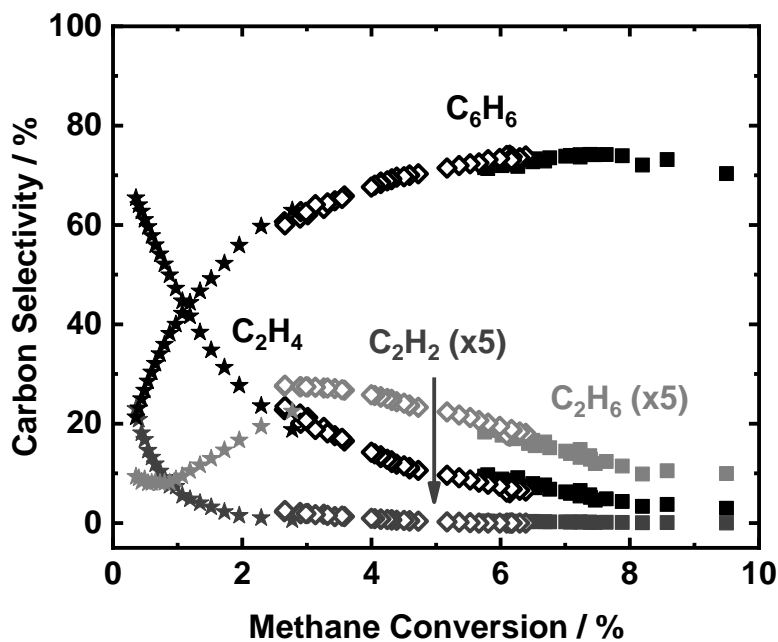


Figure 1: Carbon selectivity of DHA products as a function of methane conversion over three deactivating catalysts (Mo/Al = 0.25, Si/Al = 11.5). Reaction conditions: 973 K, ~115 kPa total pressure, 90% CH₄, 10% Ar. 1.2 g Mo/H-ZSM-5, 0.21 cm³ s⁻¹ (■); 1.0 g Mo/H-ZSM-5, 0.21 cm³ s⁻¹ (◇); 1.2 g Mo/H-ZSM-5, 2.1 cm³ s⁻¹ (★).

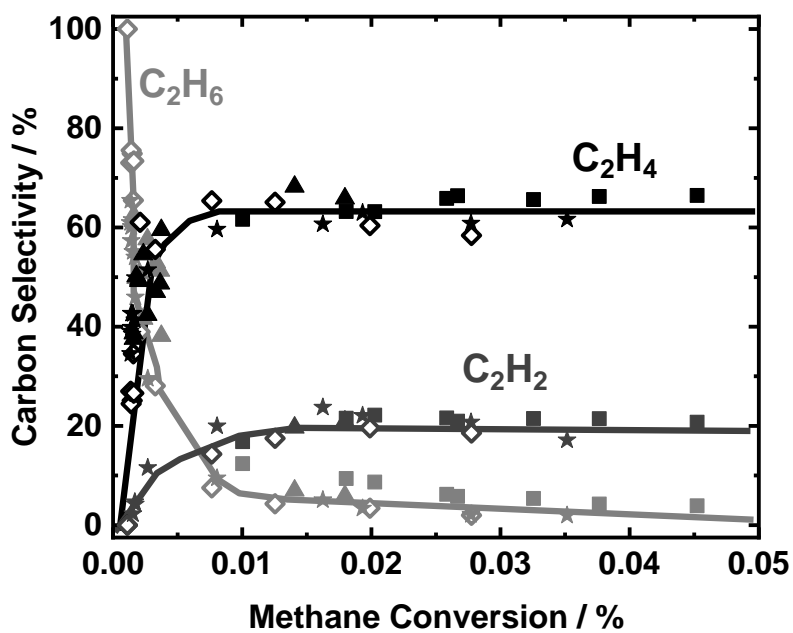
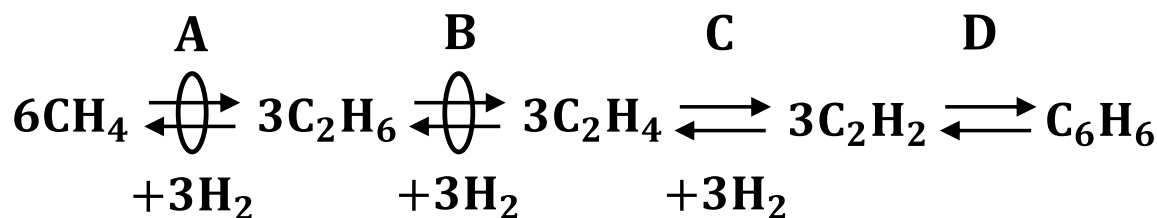


Figure 2: Carbon selectivity of DHA C₂ hydrocarbons at differential methane conversion over four deactivating catalysts (Mo/Al = 0.25, Si/Al = 11.5). Reaction conditions: 973 K, ~115 kPa total pressure, 90% CH₄, 10% Ar, 2.1 cm³ s⁻¹. 0.025 g Mo/H-ZSM-5 (◇); 0.025 g Mo/H-ZSM-5 (★); 0.250 g Mo/H-ZSM-5 (■); 0.100 g Mo/H-ZSM-5 (▲).

The selectivity of C₂ hydrocarbons as methane conversion, *f*, approaches zero (< 0.05%) is shown in Figure 2. The congruence of selectivity profiles for each C₂ across four catalyst samples again demonstrates deactivation is non-selective and evinces the reproducibility of the presented data. The asymptotic approach of C₂H₆ selectivity to 100% as *f* → 0 in Figure 2 reveals ethane is the sole primary stable gas-phase product. Several investigations propose ethylene is the primary product of methane DHA per observations that (i) ethylene selectivity increases with space velocity [4,8,32], reaction time (i.e. extent of deactivation) [4,8,32], and reaction temperature [33]; and (ii) ethylene aromatization over H-ZSM-5 gives similar product distribution to methane DHA on Mo/ZSM5 materials [3]. Fig. 2 demonstrates ethylene and acetylene selectivities approach zero as methane conversion decreases from 0.05% to 0%; concurrently, ethane selectivity approaches 100%. Zero initial selectivity of ethylene and acetylene eliminates the possibility of C₂H₄ or C₂H₂ formation from direct C-C coupling of CH₂ or CH fragments from methane (i.e. $2\text{CH}_4 \rightarrow 2\text{CH}_x + (2 - \frac{1}{2}x)\text{H}_2 \rightarrow \text{C}_2\text{H}_{2x} + (2 - \frac{1}{2}x)\text{H}_2$; *x* = 1, 2). Ethylene and acetylene are necessarily sequential pyrolysis products formed from dehydrogenation of ethane or coupling of ethane-derived surface fragments.

From conversion-selectivity profiles in Figs. 1 and 2 we propose methane DHA to benzene proceeds via a single-path series reaction depicted in Scheme 1.

Scheme 1. Proposed Methane DHA Reaction Pathway^a



^aMethane, ethane, and ethylene form a quasi-equilibrated pool catalyzed by carbidic Mo sites for sufficient contact-times ($> 7 \text{ mol}_{\text{Mo}} \text{ s mol}_{\text{CH}_4}^{-1}$). Subsequent ethylene dehydrogenation to acetylene is proposed to occur over carbidic Mo sites and acetylene aromatization to benzene may be catalyzed by Mo or zeolitic Brønsted acid sites.

The rank of ethane dehydrogenation products is evident in Fig. 3 which shows total approach to equilibrium, Z , of steps A-D (Scheme 1). Total approach to equilibrium for global gas-phase reaction or elementary step i in a series reaction is calculated as

$$Z_i = \frac{1}{K_{\text{eq},i}} \prod_{j=\text{species}} P_j^{v_{ij}} \quad (1)$$

where P_j is the partial pressure of species j divided by 1 bar (reference pressure), v_{ij} is the stoichiometric coefficient of species j in step i , and $K_{\text{eq},i}$ is the equilibrium constant of step i . By global gas-phase reaction we mean the interconversion between stable gas-phase species (e.g. $2\text{CH}_4 \rightleftharpoons \text{C}_2\text{H}_6 + \text{H}_2$) resultant from a sequence of elementary steps. In this work we calculate Z_i on a six carbon atom basis (e.g. $Z = P_{\text{C}_6\text{H}_6} P_{\text{H}_2}^9 (P_{\text{CH}_4}^6 K_{\text{eq}})^{-1}$ for overall reaction $6\text{CH}_4 \rightleftharpoons \text{C}_6\text{H}_6 + 9\text{H}_2$) [34]. The precedent in the literature is to report Z on a one carbon atom basis (i.e. for overall reaction $\text{CH}_4 \rightleftharpoons 1/6 \text{C}_6\text{H}_6 + 3/2 \text{H}_2$) [6,23,24]; however, this basis requires stoichiometric numbers of elementary steps to be less than unity to correctly calculate approach to equilibrium of elementary steps (*vide infra*) which we seek to avoid for sake of clarity.

Principles of thermodynamics dictate for each step in a series reaction $Z \leq 1$ (i.e. that each step is either thermodynamically downhill or equilibrated). Thus, $Z_C < 1$ for $\text{C}_2\text{H}_4 \rightleftharpoons \text{C}_2\text{H}_2 + \text{H}_2$ (see Fig. 3) suggests acetylene is a dehydrogenation product of ethylene and is consistent with a

series reaction pathway wherein methane activation and C-C coupling to C_2H_6 is followed by sequential dehydrogenation to C_2H_4 and then C_2H_2 (Scheme 1).

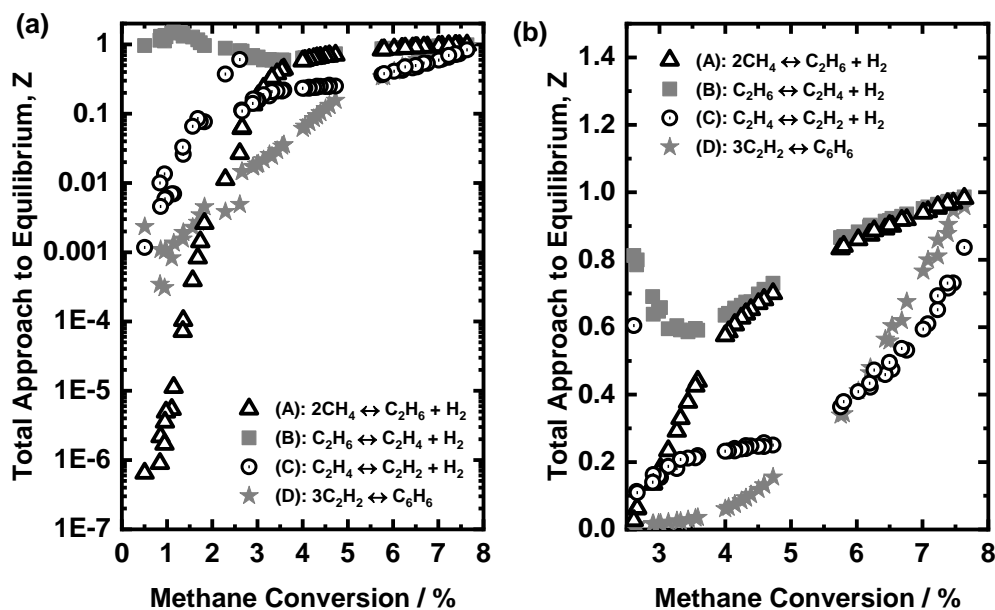


Figure 3: Total approach to equilibrium of global gas-phase DHA reactions, as listed in Scheme 1 on a one benzene molecule basis (i.e. overall reaction $6CH_4 \rightleftharpoons C_6H_6 + 9H_2$). **Figure 3a** and **3b** are the same data shown on differently scaled axes. Reaction conditions: 973 K, ~115 kPa total pressure, 90% CH_4 , 10% Ar, $0.21\text{--}2.1\text{ cm}^3\text{ s}^{-1}$, $0.1\text{--}1.2\text{ g Mo/H-ZSM-5}$.

The presence of acetylene in pseudo-steady state (PSS) quantities (*vide infra*) which deviate from $C_2H_4 \rightleftharpoons C_2H_2 + H_2$ equilibrium also implies acetylene must be consumed in subsequent oligomerization and cyclization steps. Acetylene consumption by coke formation is unlikely as carbon deposition during DHA catalysis is negligible after an initial induction period which corresponds to carburization of the pre-catalyst [7,29]; less than 0.1 C/Mo is deposited after 8.52 ks time on stream on 1.2g pre-carburized $MoC_x/H\text{-ZSM-5}$ with $0.21\text{ cm}^3\text{ s}^{-1}$ 90% methane feed [7]. Thus, $Z_C < 1$ suggests C_2H_2 is an intermediate in DHA catalysis, as has been proposed previously [35–37]. Ha et al., [36] have demonstrated acetylene aromatization over H-ZSM-5, Mo/SiO₂, and Mo/H-ZSM-5 occurs with larger rates than either ethylene or methane aromatization at 923 K and hydrocarbon and H₂ partial pressures relevant to DHA catalysis.

Acetylene aromatization rates ($144 \mu\text{mol g}^{-1} \text{h}^{-1}$) over Mo/H-ZSM-5 were 1.5 times larger than ethylene aromatization ($97 \mu\text{mol g}^{-1} \text{h}^{-1}$) and were comparable to methane aromatization rates ($131 \mu\text{mol g}^{-1} \text{h}^{-1}$), leading Ha et al., [36] to conclude benzene is formed via oligomerization of acetylene-derived vinyl cation intermediates. We also measure acetylene to benzene forward rates over Mo/H-ZSM-5 which show good agreement with forward rates of acetylene aromatization during CH_4 DHA catalysis calculated from De Donder relations (*vide infra*), shown in Section S1.

Tsai et al., [38] have demonstrated acetylene aromatization over H-ZSM-5 occurs readily without H_2 co-feed at rates far exceeding ethylene aromatization and also propose acetylene oligomerization is initiated by formation of highly reactive vinyl cations. Production of benzene from acetylene in the absence of H_2 , shown in Section S1 and reported by Tsai et al., [38] demonstrates C_2H_2 can aromatize without proceeding through an ethylcarbenium intermediate, as is proposed in existing kinetic models of DHA on Mo/H-ZSM-5 [19,20]. Detailed kinetic models of methane pyrolysis developed by Dean [39] demonstrate production of aromatics likely proceeds through acetylene as (i) vinylic products of acetylene coupling are far more reactive than allylic species resultant from ethylene dimerization and (ii) benzene synthesis from acetylene benefits from high reaction exothermicity required to overcome entropic loss during cyclization.

From this body of evidence, we conclude acetylene is likely the immediate stable gas-phase precursor to benzene in the single-path methane DHA reaction sequence (Scheme 1). However, we cannot unequivocally eliminate the possibility that aromatization proceeds through ethylene oligomerization and therefore report results for the kinetic and thermodynamic analyses to follow under this presumption in Section S2.

In what follows, we use De Donder relations to assess quantitatively the extent to which dehydrogenation and oligomerization/aromatization events in Scheme 1 control the rate and reversibility of methane DHA.

3.2 Concepts of rate- and reversibility-control of elementary steps in series reactions

3.2.1 The De Donder formalism for single-path catalytic reaction sequences

The net rate of an elementary step, r_i , is given by the difference of forward and reverse rates:

$$r_i = \vec{r}_i - \tilde{r}_i \quad (2).$$

The De Donder equation [26] relates the ratio of forward and reverse rates of elementary steps to measurable thermodynamic quantities

$$\frac{\tilde{r}_i}{\vec{r}_i} = e^{-\frac{A_i}{RT}} = z_i \quad (3),$$

where $A_i = -\Delta G_i$ is the affinity of step i at a particular extent of reaction and z_i is approach to equilibrium of the corresponding elementary step; z_i approaches zero for a fully irreversible reaction and unity for an equilibrated step. The total affinity of a global gas-phase reaction or elementary step per catalytic turnover is given by $A_{\text{tot},i} = \sigma_i A_i$ where σ_i is the stoichiometric number of global gas-phase reaction or elementary step i . Thus, the total approach to equilibrium of global gas-phase reaction or elementary step i is related to its total affinity by

$$Z_i = e^{-\frac{A_{\text{tot},i}}{RT}} \quad (4).$$

The overall affinity of a series reaction is $A_{\text{ov}} = \sum_i \sigma_i A_i = \sum_i A_{\text{tot},i}$ [34]; therefore, the overall approach to equilibrium, z_{ov} , is a product of total approach to equilibrium of all elementary steps

$$z_{\text{ov}} = \prod_{i=\text{steps}} Z_i = \prod_{i=\text{steps}} z_i^{\sigma_i} \quad (5).$$

Since reaction affinities are state functions, z_{ov} is also the product of total approach to equilibrium of all global gas-phase reactions; i.e. $z_{\text{ov}} = Z_A Z_B Z_C Z_D$ per Scheme 1.

Provided the concentration of all intermediates can be described by the pseudo-steady state hypothesis (PSSH), the forward rate of the overall reaction, \vec{R} , is related to the overall net rate, $R = r_i/\sigma_i$ for elementary steps, by

$$\vec{R} = \frac{R}{1 - \prod_i z_i} = \frac{R}{1 - z_{ov}^{1/\bar{\sigma}}} \quad (6),$$

where

$$\bar{\sigma} = \frac{\sum_i \sigma_i A_i}{\sum_i A_i} = \frac{\sum_i \ln(Z_i)}{\sum_i \ln(z_i)} \quad (7),$$

is the affinity-averaged stoichiometric number where i is an index over all elementary steps [40]. Section S3 suggests a transient definition of forward rate which extends the utility of Eq. (6) beyond exclusively cases wherein the PSSH holds.

The functional form of Eq. (6) communicates essential information regarding the manner by which elementary steps in a single-path reaction sequence affect the relationship between the overall net and forward rate.

Eq. (6) reveals the affinity-averaged stoichiometric number is critical in determining the effect of the overall reversibility, z_{ov} , to suppress overall net rates, R . Previous investigations, including our own [6], have implicitly assumed $\bar{\sigma} = 1$ in Eq. (6) without evidence or rationale. Forward rates calculated with $\bar{\sigma} = 1$ are serendipitously similar to those in this work if z_{ov} is also incorrectly length averaged, as described in Section 3.4 [6,29]. We seek to directly calculate $\bar{\sigma}$ by Eq. (7) from 0-8% methane conversion in order to correctly account for reversibility of DHA reactions and utilize Eq. (6) to calculate the forward rate of methane DHA.

Eq. (6) also shows that a single-path reaction sequence behaves as if it were a single elementary step with a reversibility, \vec{R}/R , equal to the product of the approach to equilibrium of all elementary steps

$$z_{\text{eff}} \equiv \frac{\bar{R}}{R} = \prod_{i=\text{steps}} z_i = z_{\text{ov}}^{1/\bar{\sigma}}. \quad (8).$$

The effective reversibility, z_{eff} , is the approach to equilibrium of the overall process, z_{ov} , corrected by the affinity-averaged occurrences per turnover of all intervening elementary steps, $\bar{\sigma}$. In the case of a single, rate-determining step (rds) away from equilibrium, the overall reaction behaves as if it were an elementary step that occurs $\bar{\sigma} = \sigma_{\text{rds}}$ times per turnover. Therefore, the extent to which each elementary step i exerts control on the effective approach to equilibrium, z_{eff} , is the degree of reversibility control,

$$X_{\text{ZC},i} \equiv \left(\frac{\partial \ln \ln(z_{\text{eff}})}{\partial \ln \ln(z_i)} \right)_{z_j \neq i} = \frac{A_i}{\sum_j A_j} \quad (9),$$

where j is an index over all elementary steps. Section S3 provides proof of the equivalence of the above expressions. Briefly, the first application of the natural logarithm converts z_{eff} from a product of z_i to a sum of $\ln(z_i)$, and the second application extracts the fractional influence of $\ln(z_i)$ on $\ln(z_{\text{eff}})$ and is analogous to the function of the natural logarithm in the definition of degree of rate control [41,42]. The proposed definition of degree of reversibility control is a mathematical manifestation of a metric of rate-determining character suggested by Dumesic [26] where a step is rate-determining if $z_i \sim z_{\text{eff}}$ or $A_i \sim \sum_j A_j$. We posit that X_{ZC} is not a measure of degree of rate control, but, instead, a quantitative measure of the influence of each step to determine the apparent behavior of a series reaction as an elementary step, or, equivalently, the influence of each step to determine $z_{\text{eff}} \equiv \bar{R}/R$. The result that $X_{\text{ZC}} = 0$ for a step with no rate control and $X_{\text{ZC}} = 1$ for a sole rate-determining step is a consequence of correlative, but not causal, relationship between rate control and reversibility control. In the following, we will demonstrate that X_{ZC} does not provide information about what steps control the rate, and that

agreement between X_{ZC} and Campbell's definition of degree of rate control, X_{RC} , for bookend cases $X_{RC} = X_{ZC} = 0$ and $X_{RC} = X_{ZC} = 1$ is not reflected in intermediate values of X_{ZC} and X_{RC} where control of rate and apparent elementary step behavior of the overall reaction sequence are similar but not identical. In particular, the degree of reversibility control fails to capture a key principle of series reactions: for the same approach to equilibrium, steps earlier in a single-path sequence exert more rate control than those later in the sequence. The nature of free energy as a state function manifests X_{ZC} be agnostic to the position of a step along the overall reaction coordinate, and, therefore, comparison solely of affinities of elementary steps is insufficient to evaluate rate control of each step.

3.2.2 The Degree of Rate Control in single-path catalytic reaction sequences

Cortright and Dumesic [43] demonstrate that the degree of rate control of each elementary step i , defined as

$$X_{RC,i} \equiv \left(\frac{\partial \ln R}{\partial \ln \vec{k}_i} \right)_{K_i, K_j \neq i} \quad (10),$$

where i and j are indices for elementary steps, in a single-path reaction sequence may be calculated from approach to equilibrium of elementary steps without need for any reaction rate constants, \vec{k}_i or \bar{k}_i . In particular, the authors demonstrate, by example, that for a single-path sequence of fluid-phase elementary steps with one reactant and one product in each step,

$$X_{RC,i} \equiv \left(\frac{\partial \ln R}{\partial \ln \vec{k}_i} \right)_{K_i, K_j \neq i} = \sigma_i(1 - z_i) \prod_{j=1}^{j=i-1} z_j / \sum_{i=1}^N \left[\sigma_i(1 - z_i) \prod_{j=1}^{j=i-1} z_j \right]. \quad (11),$$

where i and j are indices for elementary steps and N is the number of elementary steps in the reaction sequence [41–43]. Eq. (11) is a generalization of particular cases investigated by Cortright and Dumesic [43]. Per Eq. (11), equilibrated steps ($z_i = 1$) have no rate-determining character and the rate-determining character of fully irreversible steps ($z_i = 0$) are limited by the deviation from equilibrium of all previous steps. X_{RC} thus captures the key principle of series reactions that is missed simply by inspection of z_i : steps earlier in a reaction sequence exhibit more rate control for the same approach to equilibrium than those later in a reaction sequence – unless both steps are at equilibrium. Section 3.3 presents equations analogous to Eq. (11) which calculate degree of rate control of each step in the methane DHA reaction sequence while allowing for multiple reactants and/or products in each elementary step (e.g. unsaturated hydrocarbon and H_2 products in dehydrogenation reactions).

3.3 Rate- and reversibility-control of dehydrogenation and oligomerization in CH_4 DHA

Use of De Donder relations, degree of reversibility control, and degree of rate control is predicated on knowledge of the identity, standard Gibbs energy, and concentration of all species involved in the elementary steps which constitute the single-path methane to benzene series reaction. Coverages and energies of surface species are experimentally inaccessible; however, forward rates, X_{RC} , and X_{ZC} , may be calculated directly from thermodynamic properties, flow rates, and partial pressures of observable species provided each global gas-phase reaction contains only one rate-determining elementary step with an identifiable stoichiometric number, σ_i^* , as shown in Section S3. The approach to equilibrium of the rate-determining elementary step, z_i^* , in a global gas-phase reaction i is related to the total approach to equilibrium of the global gas-phase reaction, Z_i by

$$z_i^* = Z_i^{1/\sigma_i^*} \quad (12),$$

where all deviation from equilibrium in Z_i is attributed to z_i^* . Hence, z_i^* is the relevant thermodynamic bottleneck in each global gas-phase reaction i and σ_i^* , not σ_i , is the relevant stoichiometric number. For example, for global gas-phase reaction A, $\sigma_A^* = 6 \neq \sigma_A = 3$. Thus, if $Z_A = 0.90$, we impose $z_{A,2} = 1$, and calculate $z_{A,1} = z_A^* = Z_A^{1/6} = 0.98$. Identification of σ^* therefore permits calculation of approach to equilibrium for all non-equilibrated elementary steps in the overall series reaction and enables use of De Donder relations and degree of rate control by Eqs. (6)-(13). Fig. 4 shows approach to equilibrium, z_i^* , of rate-determining elementary steps listed in Scheme 2 within each global gas-phase reaction (A-D).

Scheme 2 posits a plausible sequence of pseudo-elementary steps consistent with Scheme 1 and the observations presented in Sections 3.1. The steps in Scheme 2 are not meant to faithfully represent the molecular events which occur during catalysis, but simply to enumerate the stoichiometric number of elementary steps which constitute gas-phase reactions A, B, C, and D in Scheme 1.

Scheme 2: Methane DHA Reaction Sequence with Pseudo-Elementary Steps

	Reaction	σ	σ^*
(A.1)	$\text{CH}_4 \rightleftharpoons \text{CH}_3 + \frac{1}{2} \text{H}_2$		6
(A.2)	$2\text{CH}_3 \rightleftharpoons \text{C}_2\text{H}_6$	3	
(A)	$2\text{CH}_4 \rightleftharpoons \text{C}_2\text{H}_6 + \text{H}_2$	3	
(B.1)	$\text{C}_2\text{H}_6 \rightleftharpoons \text{C}_2\text{H}_5 + \frac{1}{2} \text{H}_2$		3
(B.2)	$\text{C}_2\text{H}_5 \rightleftharpoons \text{C}_2\text{H}_4 + \frac{1}{2} \text{H}_2$	3	
(B)	$\text{C}_2\text{H}_6 \rightleftharpoons \text{C}_2\text{H}_4 + \text{H}_2$	3	
(C.1)	$\text{C}_2\text{H}_4 \rightleftharpoons \text{C}_2\text{H}_3 + \frac{1}{2} \text{H}_2$		3
(C.2)	$\text{C}_2\text{H}_3 \rightleftharpoons \text{C}_2\text{H}_2 + \frac{1}{2} \text{H}_2$	3	

(C)	$C_2H_4 \rightleftharpoons C_2H_2 + H_2$	3
(D.1)	$2C_2H_2 \rightleftharpoons C_4H_4$	1.5
(D.2)	$C_2H_2 + C_4H_4 \rightleftharpoons C_6H_6$	1
(D)	$3C_2H_2 \rightleftharpoons C_6H_6$	1
overall	$6CH_4 \rightleftharpoons C_6H_6 + 9H_2$	1

Bolded entries indicate rate-determining elementary steps within each gas-phase global reaction (A, B, C, and D). All σ^* are assigned on a one benzene molecule basis with overall reaction $6CH_4 \rightleftharpoons C_6H_6 + 9H_2$; σ^* for overall reaction $CH_4 \rightleftharpoons 1/6 C_6H_6 + 3/2 H_2$ are adjusted by a factor of 6.

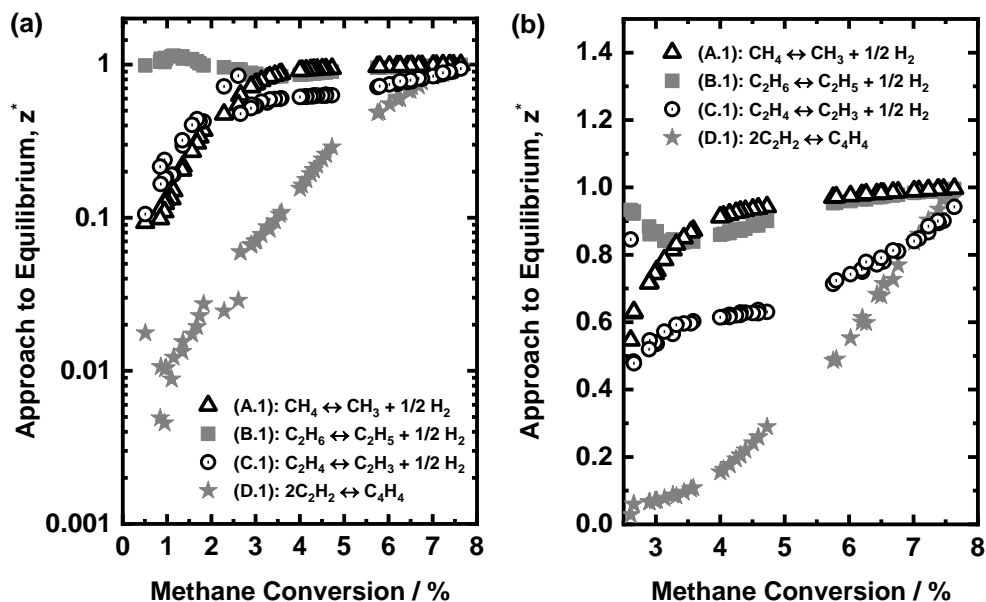


Figure 4: Approach to equilibrium of rate-determining elementary steps within each global gas-phase DHA reaction, as listed in Scheme 2. **Figure 4a** and **4b** are the same data shown on differently scaled axes. Reaction conditions: 973 K, ~115 kPa total pressure, 90% CH_4 , 10% Ar, 0.21-2.1 $cm^3 s^{-1}$. 0.1-1.2 g Mo/H-ZSM-5

Identification of σ^* for reactions B and C is trivial; $\sigma_B^* = \sigma_C^* = 3$ since the stoichiometric number of all elementary steps in alkane and alkene dehydrogenation reactions are identical [25].

Carbon numbers of methane, ethane, acetylene, and benzene bound σ_A^* by 3 and 6, and σ_D^* by 1 and 1.5. We assign $\sigma_A^* = 6$ because of the well-documented difficulty of activating C-H bonds in methane in both homogenous and catalytic pyrolysis [30,39]. Iglesia and co-workers [17]

show ethylene formation is first order in methane for contact times where ethane and ethylene are equilibrated, demonstrating methane C-H bond scission is rate-determining in ethane formation. Microkinetic models of catalytic methane DHA developed by Wong et al., [19] and Karakaya et al., [22] reproduce experimentally-observed aromatization rates and product selectivities treating methane dimerization as a pseudo-elementary first-order process, again consistent with rate-determining methane activation in step A [19,22].

We assign $\sigma_D^* = 1.5$, consistent with observed second-order kinetics in acetylene and rate-determining formation of vinylacetylene as the sole primary product during acetylene pyrolysis at temperatures below 1200 K [44,45]. We note that all σ^* are assigned on a one benzene molecule basis per Scheme 2; σ^* per a one carbon atom basis (i.e. overall reaction $\text{CH}_4 \rightleftharpoons 1/6 \text{C}_6\text{H}_6 + 3/2 \text{H}_2$) are simply adjusted by a factor of 6 to give the same elementary step reversibilities which must be agnostic to the choice of basis.

Assignment of σ_i^* and of the sequence of pseudo-elementary steps in Scheme 2 allows for derivation of X_{RC} (details in Section S3) for rate-determining elementary steps within global gas-phase reactions A-D assuming the coverage of any C_{1-4} -derived surface intermediates is much less than unity

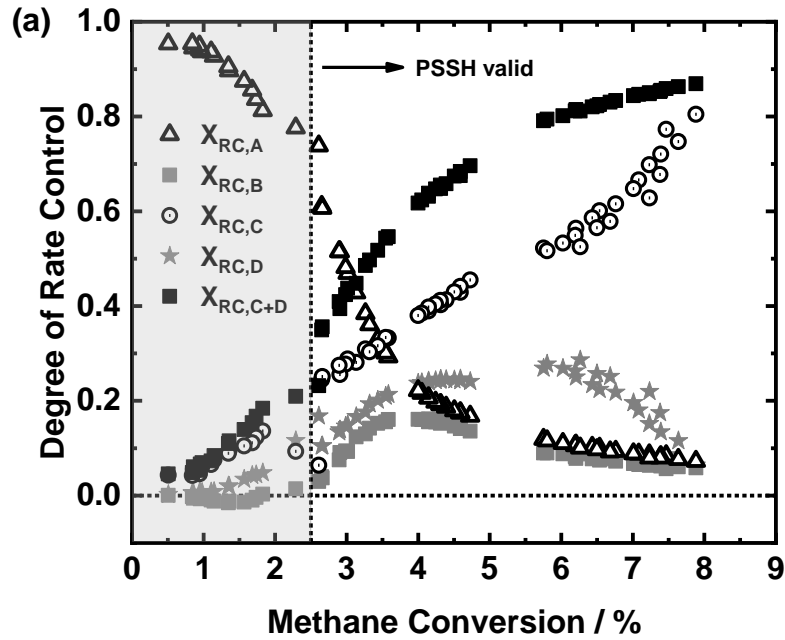
$$X_{\text{RC,A}} = \frac{\sigma_A^* (1 - z_A^*)}{\xi} \quad (13)$$

$$X_{\text{RC,B}} = \frac{\sigma_B^* z_A^* (1 - z_B^*)}{\xi} \quad (14)$$

$$X_{\text{RC,C}} = \frac{\sigma_C^* z_A^* z_B^* (1 - z_C^*)}{\xi} \quad (15)$$

$$X_{\text{RC,D}} = \frac{\sigma_D^* z_A^* z_B^* z_C^* (1 - z_D^*) \left(1 + \frac{\sigma_C^*}{\sigma_D^*} z_D^*\right)^{-1}}{\xi} \quad (16),$$

where ξ is the sum of the numerators in Eqs. (13)-(16) so that $\sum_i X_{RC,i} = 1$ [46]. Eqs. (13)-(16) are similar to Eq. (11) with an additional, nearly quantitatively negligible term in the numerator of Eq. (16) to account for multiple steps (D.1 and D.2) which consume acetylene. X_{RC} values calculated by Eqs. (13)-(16) are relatively insensitive to choice of $\sigma_A^* = 3$ or 6 and $\sigma_D^* = 1$ or 1.5 because (i) methane and ethane equilibrate for methane conversion $> 2.5\%$, and (ii) $Z_D \sim Z_D^{2/3}$ for methane conversions where step D exerts significant rate control.



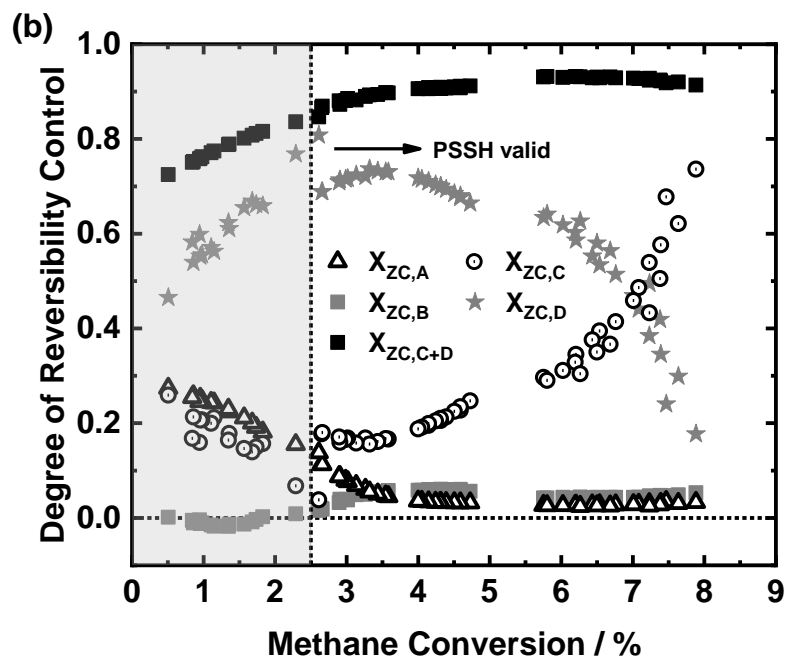


Figure 5: Degree of rate control (a) and reversibility control (b) of rate-determining elementary steps in global gas-phase reactions A-D from 0.5-8% methane conversion. Solid squares (■) are a sum of X_{ZC} or X_{RC} rate-determining elementary steps in global gas-phase reactions C and D.

Figure 5 shows X_{ZC} and X_{RC} for steps A-D calculated by Eqs. (9) and (13)-(16) using σ^* listed in Scheme 2. As we demonstrate in Section 3.4, the PSS hypothesis, from which Eqs. (13)-(16) are derived, is valid once $z_A^* \sim z_B^* \sim 1$ for $f > 2.5\%$ (see Fig. 4b). We report and assess X_{ZC} and X_{RC} for $f < 2.5\%$ as probes for rate and reversibility control of steps A-D, but stress that Eqs. (13)-(16) are not rigorously correct expressions for rate control until $f > 2.5\%$. There is a need for development of a mathematically-justified definition of transient degree of rate control which extends existing formalisms for calculation of X_{RC} [42,43,46] to regimes where single-path reactions have not yet achieved pseudo-steady state. Section S3 posits transient definitions of forward and reverse rate which extends applicability of Eq. (9), the De Donder equation, beyond the PSS regime. Discrepancies between X_{ZC} and X_{RC} as calculated by Eqs. (9) and (13)-(16) are most apparent at low conversions where methane activation is yet to equilibrate and therefore

provide qualitative insight which is corroborated quantitatively by reversibility and rate data during pseudo-steady state ($f > 2.5\%$).

For conversions less than 2.5%, methane activation is rate-controlling ($X_{RC,A} > 0.7$), but exerts little reversibility control ($X_{ZC,A} < 0.3$) as methane coupling to ethane rapidly equilibrates ($0.1 \leq z_A^* \leq 1$ from 0.5% to 3% conversion). The significant rate control of methane activation at these low contact times, despite $z_A^* \gg z_D^*$, demonstrates the disproportionate rate control of steps which occur earliest in a series reaction sequence. Once methane, ethane, and ethylene form a quasi-equilibrated pool [23,24], and therefore exert little control over rate or overall reversibility, both rate and reversibility controlling character shifts to steps involving acetylene (C and D) – suggesting steady-state DHA reactions are kinetically and thermodynamically controlled by steps between ethylene and benzene. Dominant reversibility control of steps involving acetylene is reflected by $X_{ZC,C} + X_{ZC,D} \sim 0.8$ for all contact times and manifests $\bar{\sigma}$ is essentially an affinity average of steps C and D – bounding $\bar{\sigma}$ by 2 and 3, as shown in Section S3.

For $f > 2.5\%$, $z_A^* \sim z_B^* \sim 1$ and X_{ZC} and X_{RC} for steps C and D are semi-quantitatively similar – both steps are away from equilibrium and exert both rate and reversibility control, evincing the key role of acetylene during dehydroaromatization reactions. $X_{RC,D} < X_{ZC,D}$ and $X_{RC,C} \gtrsim X_{ZC,C}$ because ethylene dehydrogenation precedes and serves as a kinetic bottleneck to acetylene dimerization. Acetylene dimerization reversibility increases along the catalyst bed, effecting increase of z_{eff} during pseudo-steady state methane DHA. As z_D^* increases beyond z_C^* , ethylene dehydrogenation becomes rate-determining and is seemingly the last step to equilibrate.

Contrary to our observations, simulation of kinetic models of methane pyrolysis performed by Iglesia and co-workers [17,47] suggest ethylene dehydrogenation to acetylene rapidly equilibrates in homogenous or catalytic reaction pathways at 1038 K. Equilibration of $C_2H_4 \rightleftharpoons$

$C_2H_2 + H_2$ at the onset of PSS in our catalytic studies would require a $\sim 2x$ adjustment in $K_{eq,D}$, resulting a maximum value of $z_D^* \gtrsim 2$ (Fig. 4b) at the largest measured contact time – which is thermodynamically forbidden [48,49]. We therefore suggest equilibrium of $C_2H_4 \rightleftharpoons C_2H_2 + H_2$ in simulation of kinetic methane pyrolysis models by Iglesia and co-workers results from lack of acetylene oligomerization pathways which kinetically couple C_2H_2 and reduce approach to equilibrium of ethylene dehydrogenation.

Crucially, the use of Eqs. (13)-(16) for the degree of rate control relies on the pseudo-steady state hypothesis – essentially that (i) the partial pressure of all carbon-containing intermediates (i.e. C_2H_x hydrocarbons) is determined arithmetically by the pressure of CH_4 , H_2 , and aromatic products, and (ii) forward rates are nearly invariant with methane conversion or contact time provided methane conversion is differential (i.e. $<10\%$) and there is no kinetic product inhibition (e.g. competitive adsorption of H_2). The first condition amounts to requiring the instantaneous rate of all C_2H_x hydrocarbons be much less than the instantaneous rate of methane consumption, as we show is true once methane, ethane, and ethylene form an equilibrated pool at contact times $>7 \text{ mol}_{M_0} \text{ s } (\text{mol}_{CH_4})^{-1}$ in Section S4. To assess the validity of the second condition, we use Eq. (6) to calculate the overall forward rate of benzene synthesis, \vec{R} , from measured net rates and $\vec{\sigma}$. These calculations, however, are complicated by the nature with which effluent streams in flow reactors carry kinetic and thermodynamic information. Exit streams in flow reactors reflect spatially-averaged net rates, but only effluent, or instantaneous, reversibilities. We address these limitations by collecting reversibility data as a function of contact time to rigorously affinity and length average z_{ov} and calculate forward benzene synthesis rates.

3.4 Affinity and length averaging in highly reversible CH_4 DHA flow reactors

Use of Eq. (6) from flow reactor data requires affinity averaging of z_{ov} by use of Eq. (7) and numerical integration of z_{ov} along the catalyst bed (i.e. spatial averaging). Spatial averaging of z_{ov} from flow reactor data is necessary because effluent flow rates inherently reflect length-averaged rates, $\langle R \rangle$, while effluent partial pressures reflect instantaneous approach to equilibrium, Z . Therefore, measured effluent, instantaneous z_{ov} must be length-averaged to capture the same information as measured effluent flow rates, i.e. length-averaged reaction rates. The inherent length-averaging of reaction rates by flow reactors is best demonstrated by integration of the PFR mole balance. The effluent flow rate of a product j in a PFR normalized by the total number of active sites, F_j , is given by

$$F_j = \frac{1}{\int_0^X dx} \cdot \int_0^X \sum_i v_{ij} R_i dx = \sum_i v_{ij} \langle R_i \rangle \quad (17),$$

where index i refers to overall reactions, x is the contact time along the catalyst bed, and X is the total contact time. Eq. (17) clearly demonstrates effluent flow data measure length-averaged reaction rates in a PFR and also holds for a dispersed packed-bed reactor with closed-closed Danckwerts boundary conditions, as shown in Section S4. The pseudo-steady state hypothesis, canonically a prerequisite of the De Donder analysis, dictates that the overall forward rate is nearly constant along the catalyst bed. Thus,

$$\bar{R}_i = \frac{\langle R_i \rangle}{\langle 1 - z_{ov,i}^{1/\bar{\sigma},i} \rangle} = \frac{1}{v_{ij}} \frac{F_j - \sum_{k \neq i} v_{kj} \langle R_k \rangle}{\langle 1 - z_{ov,i}^{1/\bar{\sigma},i} \rangle} \quad (18),$$

where indices i and k refer to overall reactions and index j refers to species j . The term $[F_j - \sum_{k \neq i} v_{kj} \langle R_k \rangle]$ in Eq. (18) generally accounts for all reactions which form or consume species j and is redacted to a simpler, particular form for the overall benzene synthesis reaction in Eq. (19). Eq. (18) is a function of only measurable quantities: effluent flow rate, effluent overall approach to equilibrium, and effluent affinity-averaged stoichiometric number – provided the

latter two are appropriately length-averaged. In the following, we calculate \vec{R} for benzene production by a particular form of Eq. (18) and show, once methane activation equilibrates, the overall forward rate of methane DHA is indeed invariant with contact time, evincing the validity of PSSH. De Donder relations used to calculate forward rate make no assumption regarding the identity or distribution of catalytic active sites and therefore are agnostic to the role of MoC_x, Brønsted acid sites, or co-catalytic entrained carbon in each step. Calculation of rate and contact time to follow normalize by active Mo atoms, as is the precedent in the literature [4,6,27,50], but this assignment of active site has no effect on validity of the De Donder formalism or the PSSH.

We collect data for calculation of $\bar{\sigma}$ and z_{ov} as a function of contact time by leveraging the non-selective nature of Mo/H-ZSM-5 deactivation during methane DHA (see Fig. 1). Retention of the catalytic properties of active sites during deactivation implies methane conversion, f , is a one-to-one function of contact time, τ [=] mol_{Mo} s (mol_{CH₄)⁻¹, provided inlet composition, reaction temperature, and total pressure are unchanged. We determine $f(\tau)$ by systematic change of contact time, or catalyst loading, during steady-state methane DHA reactions. Section S4 discusses and demonstrates that f is a one-to-one function of τ in ideal plug-flow and axially dispersed flow reactors. Section S4 shows $f(\tau)$ is a monotonic function which we fit by a piecewise polynomial expression. Determination of $f(\tau)$ permits calculation of contact time, correctly normalized by *active* Mo atoms, during deactivation of Mo/H-ZSM-5 catalysts, and, in effect, enables calculation of turnover frequencies, R [=] mol/mol_{active Mo}/s, even as the catalyst deactivates.}

Fig. 6 reports overall forward rates of benzene synthesis during methane DHA on Mo/H-ZSM-5 determined by variation of contact time both by (i) extent of catalyst deactivation and (ii) change of catalyst loading in a catalog of steady-state DHA reactions with identical total flow

rate. We take the net rate of benzene synthesis to be the sum of benzene and naphthalene flow rates since naphthalene constitutes significant carbon selectivity and is presumed to be formed from a single benzene molecule and addition of smaller hydrocarbons. Explicitly, the forward rate of the methane to benzene single-path reaction sequence is

$$\vec{R} = \frac{\langle R \rangle}{\langle 1 - z_{ov}^{1/\bar{\sigma}} \rangle} = \frac{F_{C_6H_6} + F_{C_{10}H_8}}{\langle 1 - z_{ov}^{1/\bar{\sigma}} \rangle} \quad (19).$$

Fig. 6 shows forward rates reach a steady value at the same contact time as $z_A^* \sim z_B^* \sim 1$, evincing the validity of the PSSH and demonstrating the sole inhibiting effect of H_2 liberated in DHA reactions is thermodynamic in nature. Fortuitously, our previous calculations of constant forward benzene rates [6,29] are similar to those in this work due to a balance of incorrect length averaging and affinity averaging which overestimate and underestimate forward rates, respectively (see Section S5). Section S5 also shows deviation from PSSH for $\tau < 7 \text{ mol}_{M_0} \text{ s}$ ($\text{mol}_{CH_4})^{-1}$ has little influence on calculation of forward rates as, at these low contact times, $\langle z_{eff} \rangle \ll 1$ and $R \sim \vec{R}$.

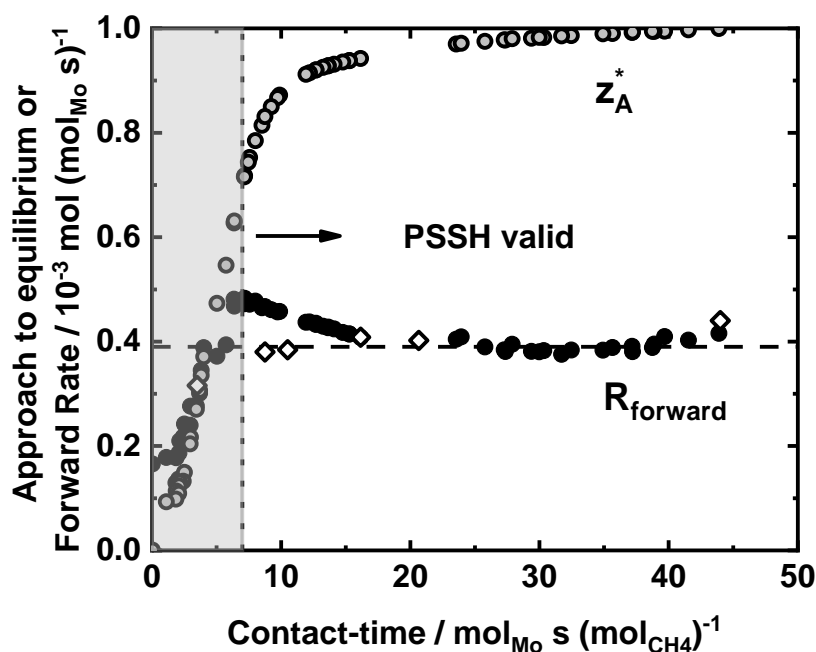


Figure 6: Approach to equilibrium of methane activation as a function of contact time varied by extent of deactivation (\circ ; $T = 973$ K), and forward rates of benzene synthesis [=] $\text{mol}_{\text{benzene}} (\text{mol}_{\text{Mo}} \text{s})^{-1}$ as a function of contact time varied by extent of deactivation (\bullet ; $T = 973$ K) and catalyst loading during steady-state catalysis (\diamond ; $T = 973$ K).

4. Conclusion

Mo-modified H-ZSM-5 catalyzes methane dehydroaromatization via a single-path series reaction wherein initial methane activation and C-C coupling to ethane is followed by sequential dehydrogenation to ethylene and acetylene, the immediate stable gas-phase intermediate to benzene formation. Elucidation of the DHA reaction network and quantification of reversibility of intervening dehydrogenation and oligomerization reactions is achieved by change of effective contact time by extent of “non-selective” deactivation. The “non-selective” nature of deactivation is confirmed by congruence of conversion-selectivity curves and permits probe of axial rate and reversibility profiles after determination of $f(\tau)$, the one-to-one function between methane conversion and contact time. Methane, ethane, and ethylene form a quasi-equilibrated pool at contact times beyond $7 \text{ mol}_{\text{Mo}} \text{s} (\text{mol}_{\text{CH}_4})^{-1}$, resulting in a pseudo-steady state methane

aromatization pathway with both rate- and reversibility-determining steps, C₂H₄ dehydrogenation and C₂H₂ dimerization, involving acetylene – identified to be a key reactive intermediate in DHA.

Rate control and reversibility control of intervening steps is quantified by the degree of reversibility control, defined herein for the first time, and the degree of rate control which account for the stoichiometric number of rate-determining elementary steps within each global gas-phase reaction. The degree of reversibility control is necessary for rigorous affinity averaging of overall reversibility of the methane-to-benzene single-path reaction, but is insufficient to predict the rate-control of each step as reaction affinities are thermodynamically-determined state functions inherently limited in their ability to describe rates of path-dependent reaction sequences. Congruence of degree of rate control and degree of reversibility control for bookend cases is not reflected at intermediate contact times and highlights the need for the degree of rate control to identify rate-determining steps in reversible series reactions with multiple steps away from equilibrium. Axial degree of reversibility control profiles are nonetheless critically useful to determine the affinity-averaged stoichiometric number along the catalyst bed, as is necessary to calculate forward DHA rates.

Forward benzene rates determined from formalisms of affinity averaging and length averaging are invariant with contact-time once methane, ethane, and ethylene equilibrate and evince the validity of the pseudo-steady-state hypothesis upon which conventional definitions of degree of rate control and the De Donder formalism are predicated. Unchanged forward aromatization rates at contact times beyond 7 mol_{Mo} s (mol_{CH₄})⁻¹ set kinetic limits to methane aromatization on Mo/H-ZSM-5 catalysts and motivate investigations to (i) overcome thermodynamic barriers set by reaction endothermicity and (ii) identify and eliminate

mechanisms of catalyst deactivation to progress technical development of direct methane valorization to ethylene and aromatics.

Acknowledgements

The authors thank Professor James W. Harris for helpful technical discussions. This work was funded by the US Department of Energy, Office of Basic Energy Science, Catalysis Science Program (Award DE-SC00019028).

References

- [1] A.I. Olivos-Suarez, A. Gnes Szécsényi, E.J.M. Hensen, J. Ruiz-Martinez, E.A. Pidko, J. Gascon, Strategies for the Direct Catalytic Valorization of Methane Using Heterogeneous Catalysis: Challenges and Opportunities, *ACS Catal.* 6 (2016) 2965–2981.
- [2] P. Schwach, X. Pan, X. Bao, Direct Conversion of Methane to Value-Added Chemicals over Heterogeneous Catalysts: Challenges and Prospects, *Chem. Rev.* 117 (2017) 8497–8520.
- [3] D. Wang, J.H. Lunsford, M.P. Rosynek, Catalytic conversion of methane to benzene over Mo/ZSM-5, *Top. Catal.* 3 (1996) 289–297.
- [4] B.M. Weckhuysen, D. Wang, M.P. Rosynek, J.H. Lunsford, Conversion of Methane to Benzene over Transition Metal Ion ZSM-5 Zeolites II. Catalyst Characterization by X-Ray Photoelectron Spectroscopy, *J. Catal.* 175 (1998) 347–351.
- [5] Y.-H. Kim, R.W. Borry III, E. Iglesia, Catalytic Properties of Mo/HZSM-5 for CH₄ Aromatization, *J. Ind. Eng. Chem.* 6 (2000) 72–78.
- [6] J. Bedard, D.-Y. Hong, A. Bhan, CH₄ dehydroaromatization on Mo/H-ZSM-5: 1. Effects of co-processing H₂ and CH₃COOH, *J. Catal.* 306 (2013) 58–67.
- [7] A. Kumar, K. Song, L. Liu, Y. Han, A. Bhan, Absorptive hydrogen scavenging for

- enhanced aromatics yield during non-oxidative methane dehydroaromatization on Mo/H-ZSM-5 catalysts, *Angew. Chemie Int. Ed.* 130 (2018) 15803–15808.
- [8] E. Iglesia, R.W. Borry III, A. Huffsmith, Y.H. Kim, J.A. Reimer, Structure and Density of Mo and Acid Sites in Mo-Exchanged H-ZSM5 Catalysts for Nonoxidative Methane Conversion, *J. Phys. Chem. B.* 103 (1999) 5787–5796.
- [9] W. Li, G.D. Meitzner, R.W.B. III, E. Iglesia, Raman and X-Ray Absorption Studies of Mo Species in Mo/H-ZSM5 Catalysts for Non-Oxidative CH₄ Reactions, *J. Catal.* 191 (2000) 373–383.
- [10] Y.-H. Kim, R.W. Borry III, E. Iglesia, Genesis of methane activation sites in Mo-exchanged H-ZSM-5 catalysts, *Microporous Mesoporous Mater.* 35–36 (2000) 495–509.
- [11] Y.-H. Kim, R.W. Borry III, E. Iglesia, Surface Structure of Mo/H-ZSM5 Catalyst for CH₄ Activation, *Appl. Chem.* 3 (1999) 368–371.
- [12] J. Bedard, D.-Y. Hong, A. Bhan, Co-processing CH₄ and oxygenates on Mo/HZSM5: 2. CH₄-CO₂ and CH₄-HCOOH mixtures, *Phys. Chem. Chem. Phys.* 15 (2013) 12173.
- [13] I. Vollmer, B. Van Der Linden, S. Ould-Chikh, A. Aguilar-Tapia, I. Yarulina, E. Abou-Hamad, Y.G. Sneider, A.I. Olivos Suarez, J.-L. Hazemann, F. Kapteijn, J. Gascon, On the dynamic nature of Mo sites for methane dehydroaromatization, *Chem. Sci.* 9 (2018) 4801–4807.
- [14] I. Vollmer, N. Kosinov, Á. Szécsényi, G. Li, I. Yarulina, E. Abou-Hamad, A. Gurinov, S. Ould-Chikh, A. Aguilar-Tapia, J.-L. Hazemann, E. Pidko, E. Hensen, F. Kapteijn, J. Gascon, A site-sensitive quasi-in situ strategy to characterize Mo/HZSM-5 during activation, *J. Catal.* 370 (2019) 321–331.
- [15] I. Lezcano-González, R. Oord, M. Rovezzi, P. Glatzel, S.W. Botchway, B.M.

- Weckhuysen, A.M. Beale, Molybdenum Speciation and its Impact on Catalytic Activity during Methane Dehydroaromatization in Zeolite ZSM-5 as Revealed by Operando X-Ray Methods, *Angew. Chemie Int. Ed.* 55 (2016) 5215–5219.
- [16] J. Gao, Y. Zheng, J.M. Jehng, Y. Tang, I.E. Wachs, S.G. Podkolzin, Identification of molybdenum oxide nanostructures on zeolites for natural gas conversion, *Sci.* 348 (2015) 686–690.
- [17] L. Li, R.W. Borry, E. Iglesia, Design and optimization of catalysts and membrane reactors for the non-oxidative conversion of methane, *Chem. Eng. Sci.* 57 (2002) 4595–4604.
- [18] M.C. Iliuta, I. Illiuta, B.P.A. Grandjean, F. Larachi, Kinetics of Methane Nonoxidative Aromatization over Ru-Mo/HZSM-5 Catalyst, *Ind. Eng. Chem. Res.* 42 (2003) 3203–3209.
- [19] K.S. Wong, J.W. Thybaut, E. Tangstad, M.W. Stöcker, G.B. Marin, Methane aromatisation based upon elementary steps: Kinetic and catalyst descriptors, *Microporous Mesoporous Mater.* 164 (2012) 302–312.
- [20] C. Karakaya, S.H. Morejudo, H. Zhu, R.J. Kee, Catalytic Chemistry for Methane Dehydroaromatization (MDA) on a Bifunctional Mo/HZSM-5 Catalyst in a Packed Bed, *Ind. Eng. Chem. Res.* 55 (2016) 9895–9906.
- [21] B. Kee, C. Karakaya, H. Zhu, S. DeCaluwe, R.J. Kee, The Influence of Hydrogen-Permeable Membranes and Pressure on Methane Dehydroaromatization in Packed-Bed Catalytic Reactors, *Ind. Eng. Chem. Res.* 56 (2017) 3551–3559.
- [22] C. Karakaya, H. Zhu, R.J. Kee, Kinetic modeling of methane dehydroaromatization chemistry on Mo/Zeolite catalysts in packed-bed reactors, *Chem. Eng. Sci.* 123 (2015) 474–486.

- [23] H.S. Lacheen, E. Iglesia, Stability, structure, and oxidation state of Mo/H-ZSM-5 catalysts during reactions of CH₄ and CH₄-CO₂ mixtures, *J. Catal.* 230 (2005) 173–185.
- [24] Y. Song, Y. Xu, Y. Suzuki, H. Nakagome, X. Ma, Z.-G. Zhang, The distribution of coke formed over a multilayer Mo/HZSM-5 fixed bed in H₂ co-fed methane aromatization at 1073 K: Exploration of the coking pathway, *J. Catal.* 330 (2015) 261–272.
- [25] R. Gounder, E. Iglesia, Catalytic hydrogenation of alkenes on acidic zeolites: Mechanistic connections to monomolecular alkane dehydrogenation reactions, *J. Catal.* 277 (2011) 36–45.
- [26] J.A. Dumesic, Analyses of Reaction Schemes Using De Donder Relations, *J. Catal.* 185 (1999) 496–505.
- [27] H.S. Lacheen, E. Iglesia, Isothermal activation of Mo₂O₅²⁺-ZSM-5 precursors during methane reactions: effect of reaction products on structural evolution and catalytic properties, *Phys. Chem. Chem. Phys.* 7 (2005) 538–547.
- [28] J. Bedard, D.-Y. Hong, A. Bhan, C to H effective ratio as a descriptor for coprocessing light oxygenates and CH₄ on Mo/HZSM-5, *RSC Adv.* 4 (2014) 49446.
- [29] N.K. Razdan, A. Kumar, A. Bhan, Controlling kinetic and diffusive length-scales during absorptive hydrogen removal in methane dehydroaromatization on MoC_x/H-ZSM-5 catalysts, *J. Catal.* 372 (2019) 370–381.
- [30] R.W. Borry, E.C. Lu, Y.-H. Kim, E. Iglesia, Non-oxidative catalytic conversion of methane with continuous hydrogen removal, *Nat. Gas Convers.* V. 119 (1998) 403–410.
- [31] B.L. Foley, B.A. Johnson, A. Bhan, A Method for Assessing Catalyst Deactivation: A Case Study on Methanol-to-Hydrocarbons Conversion, *ACS Catal.* 9 (2019) 7065–7072.
- [32] B.M. Weckhuysen, D. Wang, M.P. Rosynek, J.H. Lunsford, Conversion of Methane to

- Benzene over Transition Metal Ion ZSM-5 Zeolites I. Catalytic Characterization, *J. Catal.* 175 (1998) 338–346.
- [33] V. Ramasubramanian, H. Ramsurn, G.L. Price, Methane dehydroaromatization – A study on hydrogen use for catalyst reduction, role of molybdenum, the nature of catalyst support and significance of Bronsted acid sites, *J. Energy Chem.* 34 (2019) 20–32.
- [34] M. Boudart, G. Djéga-Mariadassou, *Kinetics of Heterogenous Catalytic Reactions*, 1st ed., Princeton University Press, Princeton, 1984.
- [35] P. Meriaudeau, L. V Tiep, V.T.T. Ha, C. Naccache, G. Szabo, Aromatization of methane over Mo/H-ZSM-5 catalyst: on the possible reaction intermediates, *J. Mol. Catal. A Chem.* 144 (1999) 469–471.
- [36] V.T.T. Ha, L. V. Tiep, P. Meriaudeau, C. Naccache, Aromatization of methane over zeolite supported molybdenum: active sites and reaction mechanism, *J. Mol. Catal. A Chem.* 181 (2002) 283–290.
- [37] P. Mériaudeau, V.T.T. Ha, L. Van Tiep, Methane aromatization over Mo/H-ZSM-5: on the reaction pathway, *Catal. Letters.* 64 (2000) 49–51.
- [38] P. Tsai, J.R. Anderson, Reaction of Acetylene over ZSM-5-Type Catalysts, *J. Catal.* 80 (1983) 207–214.
- [39] A.M. Dean, Detailed Kinetic Modeling of Autocatalysis in Methane Pyrolysis, *J. Phys. Chem.* 94 (1990) 1432–1439.
- [40] M. Boudart, Some Applications of the Generalized De Donder Equation to Industrial Reactions, *Ind. Eng. Chem. Fundam.* 25 (1986) 70–75.
- [41] C.T. Campbell, Finding the Rate-Determining Step in a Mechanism Comparing DeDonder Relations with the “Degree of Rate Control,” *J. Catal.* 204 (2001) 520–524.

- [42] C. Stegelmann, A. Andreasen, C.T. Campbell, Degree of Rate Control: How Much the Energies of Intermediates and Transition States Control Rates, *J. Am. Chem. Soc.* 131 (2009) 8077–8082.
- [43] R.D. Cortright, J.A. Dumesic, Kinetics of Heterogeneous Catalytic Reactions: Analysis of Reaction Schemes, *Adv. Catal.* 46 (2001) 161–264.
- [44] C.F. Cullis, N.H. Franklin, The pyrolysis of acetylene at temperatures from 500 to 1000 °C, *Proc. R. Soc. London. Ser. A. Math. Phys. Sci.* 280 (1964) 139–152.
- [45] S.W. Benson, Radical processes in the pyrolysis of acetylene, *Int. J. Chem. Kinet.* 24 (1992) 217–237.
- [46] B.L. Foley, A. Bhan, Personal Communication, (2019).
- [47] L. Li, R.W. Borry, E. Iglesia, Reaction-transport simulations of non-oxidative methane conversion with continuous hydrogen removal: homogeneous-heterogeneous reaction pathways, *Chem. Eng. Sci.* 56 (2001) 1869–1881.
- [48] H.M. Spencer, Empirical Heat Capacity Equations of Gases and Graphite, *Ind. Eng. Chem.* 40 (1948) 2152–2154.
- [49] C.L. Yaws, Chapter 1 - Physical Properties – Organic Compounds, in: *Yaws Handb. Phys. Prop. Hydrocarb. Chem.*, 2nd ed., Elsevier Inc., Waltham, MA, 2015: pp. 1–683.
- [50] S. Liu, L. Wang, R. Ohnishi, M. Ichikawa, Bifunctional Catalysis of Mo/HZSM-5 in the Dehydroaromatization of Methane to Benzene and Naphthalene XAFS/TG/DTA/MASS/FTIR Characterization and Supporting Effects, *J. Catal.* 181 (1999) 175–188.